

Antiangiogenic Activity of Compounds Isolated from *Anarrhinum pedatum*

Khadidja Aya Beladjila,[†] Djemaa Berrehal,[†] Zahia Kabouche,[†] Maria Paola Germanò,[‡] Valeria D'Angelo,[‡] Nunziatina De Tommasi,[§] Felicia D'Andrea,[⊥] Alessandra Braca,^{*,⊥,||} and Marinella De Leo^{⊥,||}

[†]Laboratoire d'Obtention des Substances Thérapeutiques (LOST), Département de Chimie, Université des Frères Mentouri-Constantine, Route de Ain El-Bey, 25000 Constantine, Algeria

[‡]Dipartimento di Scienze Chimiche, Biologiche, Farmaceutiche e Ambientali, Università degli Studi di Messina, Polo Universitario SS. Annunziata, 98168 Messina, Italy

[§]Dipartimento di Farmacia, Università degli Studi di Salerno, via Giovanni Paolo II 132, 84084 Fisciano (SA), Italy

[⊥]Dipartimento di Farmacia, Università di Pisa, via Bonanno 33, 56126 Pisa, Italy

^{||}Centro Interdipartimentale di Ricerca "Nutraceutica e Alimentazione per la Salute", Università di Pisa, via del Borghetto 80, 56124 Pisa, Italy

Dedicated to Dr. Rachel Mata, National Autonomous University of Mexico, Mexico City, Mexico, and Dr. Barbara N. Timmerman, University of Kansas, for their pioneering work on bioactive natural products.

ABSTRACT: Ten new iridoid glycosides (**1-10**) and two new monoterpenoids (**11** and **12**), together with nine known compounds (**13-21**), were isolated from the *n*-butanol extract of the aerial parts of *Anarrhinum pedatum*. The structural characterization of all compounds was performed by spectroscopic analysis, including 1D and 2D NMR, and HRESIMS experiments. The isolates were assayed for their antiangiogenic activity by two in vivo models, using zebrafish embryos and chicken chorioallantoic membranes (CAMs). The results showed that among the new compounds, 6'-*O*-menthiafoloylmussaenosidic acid-11-(5-*O*- β -D-fructopyranosyl) ester (**9**), exhibited the most potent antiangiogenic activity in both the zebrafish embryos and CAM assays, reducing the growth of blood vessels. Antiangiogenic effects were also observed for the known compounds, 6-*O*-nerol-8-oyl-antirrinoside (**13**), antirrinoside (**14**), 6-*O*-*trans* and *cis-p*-coumaroyl antirrinoside (**15**), and (6*S*)-2*E*-2,6-dimethyl-6-hydroxyocta-2,7-dienoic acid β -glucopyranosyl ester (**18**).

Anarrhinum (family Plantaginaceae, formerly Scrophulariaceae) is a genus of flowering plants that occurs in temperate and subtropical regions.^{1,2} The major secondary metabolites produced by this genus are iridoid glycoside esters,^{3,4} although to date only a few species have been investigated chemically. The function of iridoids in plants has been related to plant defense and insect adaptation, however, they also exhibit a wide range of pharmacological activities such as anti-inflammatory, antineoplastic, antidiabetic, and neuroprotective effects.^{5,6} In the course of a continuing study on Algerian plants,^{7,8} it was found that several iridoids such as asperuloside, geniposidic acid, and iridoid V1 exhibited antiangiogenic activities.⁹ Angiogenesis is the growth of new blood vessels to ensure wound healing, reproduction, and developments of cells, playing an important role in many physiological processes. However, unregulated angiogenesis is still involved in inflammatory diseases, tumor growth, and metastasis. Thus, the inhibition of angiogenesis is considered a promising strategy against neoplastic growth and for the prevention of inflammatory disorders and nowadays there is a growing interest to discover new angiomodulators from natural sources. Accordingly, a phytochemical investigation was conducted of *Anarrhinum pedatum* Desf., a herbaceous plant with a flower-bearing stalk, as obtained in the northeastern region of Algeria.^{10,11}

In this contribution, we report for the first time a study on the *A. pedatum* aerial parts, leading to the isolation and structural characterization of twelve new compounds, including ten iridoid glycosides (**1-10**) and two monoterpenoids (**11** and **12**), together with nine known compounds (**13-21**). The isolates were assayed for their inhibitory effects on neovascularization by two in vivo models, with zebrafish embryos and chicken chorioallantoic membranes, (CAMs), as to be considered new potential antiangiogenic agents.

RESULTS AND DISCUSSION

The aerial parts of *A. pedatum* were defatted with *n*-hexane and then extracted with solvents of increasing polarity. The MeOH extract was partitioned between *n*-BuOH and H₂O to give a *n*-

BuOH residue. This extract was subjected to Sephadex LH-20, CPC, and RP-HPLC separations to afford in pure form twelve new (**1-12**) and nine known compounds (**13-21**).

The molecular formula of compound **1** was determined as C₃₅H₅₀O₁₄ by HRESIMS, showing a sodiated molecular ion peak at m/z 717.3090 for [M + Na]⁺ and a protonated ion peak at m/z 695.3278, and supported by the NMR spectra. In the ESIMS, fragments obtained in the positive mode, at m/z 699 [M + Na - 18]⁺ and 551 [M + Na - 166]⁺, revealed the losses of a water molecule and a C₁₀ ester side chain. The ¹H and ¹³C NMR spectra of compound **1** (Table 1) showed the presence of a group of characteristic signals for a C₉-type iridoid skeleton at δ 1.49 (s, Me-10)/16.0 (C-10), 2.86 (br s, H-9)/49.4 (C-9), 3.63 (d, $J = 2.0$ Hz, H-7)/64.0 (C-7), 5.15 (d, $J = 2.0$ Hz, H-6)/76.5 (C-6), 5.48 (d, $J = 6.5$ Hz, H-4)/102.4 (C-4), 5.82 (d, $J = 2.2$ Hz, H-1)/93.5 (C-1), 6.59 (d, $J = 6.5$ Hz, H-3)/145.6 (C-3), and of one β -glucopyranose moiety, having anomeric proton at δ 4.68 (d, $J = 7.8$ Hz). These data led the iridoid portion of **1** to be identified as antirrinocide.^{12,13} The additional NMR signals could be clearly attributed to two foliamenthoyl moieties³ with the help of 1D-TOCSY, DQF-COSY, HSQC, and HMBC experiments, which showed correlation peaks between δ 2.19 (H₂-5'' and H₂-5''') and δ 23.0 (C-10'' and C-10'''), 126.0 (C-7'' and C-7'''), and 137.8 (C-6'' and C-6'''); δ 2.31 (H₂-4'' and H₂-4''') and δ 128.3 (C-2'' and C-2'''), 142.6 (C-3''), and 143.0 (C-3'''); δ 4.09 (H₂-8'' and H₂-8''') and δ 126.0 (C-7'' and C-7'''); δ 6.69 (H-3''') and δ 12.0 (C-9''') and 167.8 (C-1'''), and δ 6.78 (H-3'') and δ 13.0 (C-9'') and 167.3 (C-1''). Other HMBC correlations between 4.68 (H-1'_{glc}) and 93.5 (C-1) and 5.15 (H-6) and 167.8 (C-1''') indicated the substitution sites of the glucose unit and one of the foliamenthoyl moieties. The other foliamenthoyl unit was located at C-5 of the iridoid skeleton as a result of its downfield shift from 73.4 ppm in 6-*O*-nerol-8-oylantirrinocide (6-foliamenthoylantirrinocide)³ or 74.5 ppm in antirrinocide¹³ to 80.3 ppm in **1**. The configuration of the sugar unit was assigned after hydrolysis of **1** with 1 N HCl followed by GC analysis of the trimethylsilylated sugars by a chiral column. This procedure was used to determine the absolute configuration of the sugar units of all new compounds. From the above results, compound **1** was identified as 5,6-*O*-difoliamenthoylantirrinocide.

The molecular formula of compound **2** (C₃₅H₅₀O₁₅) was determined by its ¹³C NMR data and HRESIMS ([M + H]⁺ ion at *m/z* 711.3229), varying from that of **1** for 16 amu. Comparison of the NMR spectroscopic data of **2** with those of **1** (Table 1) showed these compounds to differ only in the iridoid moiety, having in **2** a hydroxymethylene group at C-8 (δ_H 3.56 and 4.16, both d, *J* = 13.0 Hz) instead of a methyl group (δ_H 1.49, s). The iridoid glucoside portion of **2** was thus characterized as macfadienoside¹⁴ instead of antirrinoside in **1**.¹² Thus, compound **2** was identified as 5,6-*O*-difoliamenthoylmacfadienoside.

The HRESIMS of compound **3** in the positive-ion mode showed a [M + Na]⁺ sodiated molecular ion peak at *m/z* 717.3083, corresponding to a molecular formula of C₃₅H₅₀O₁₄, and hence was assigned as an isomer of **1**. Two main fragments at *m/z* 533.1976 [M + Na – 184]⁺ and 349.0883 [M + Na – 184 – 184]⁺, due to the subsequent loss of two C₁₀ ester moieties, were also observed. The signals in the 1D and 2D NMR spectra (Table 1) of **3** were superimposable on those of **1** except for an ester moiety identified as a menthiafoloyl unit from signals at δ 1.29 (H-10'')/27.4 (C-10''), 1.80 (H-9'')/12.0 (C-9''), 1.59 (H₂-5'')/41.5 (C-5''), 2.23 (H₂-4'')/24.1 (C-4''), 5.27 (H-8a'')-5.07 (H-8b'')/112.1 (C-8''), 5.93 (H-7'')/145.5 (C-7''), 6.71 (H-3'')/144.3 (C-3''), 71.8 (C-6''), 125.1 (C-2''), and 166.0 (C-1''),¹⁵ instead of a foliamenthoyl unit. The assignments of all proton and carbon signals were deduced from a combined analysis of 1D and 2D NMR experiments. The HMBC spectrum indicated the substitution site of the menthiafoloyl moiety from the cross peak between δ 5.15 (H-6) and 165.7 (C-1''). Unfortunately, no cross peak was evident that correlated the menthiafoloyl moiety with C-5, but again the downfield shift of C-5 (79.0 ppm) clearly indicated that this was the substitution site. From these results, the structure of compound **3** was determined as 5-*O*-menthiafoloyl-6-*O*-foliamenthoylantirrinoside.

Compound **4** (C₃₅H₅₀O₁₅) showed a [M + Na]⁺ peak at *m/z* 733.3040 in the positive HRESIMS, and hence was assigned as an isomer of **2**. The HRESIMS/MS displayed a fragment peak at *m/z* 549.1961 [M + Na – 184]⁺ similar to that of the previous compounds **1-3**. The spectroscopic data (Table 1) of the ester and sugar moieties were identical to those of **3**, while the iridoid portion was

superimposable with that of **2** and characterized as macfadienoside.¹⁴ Consequently, compound **4** was deduced as 5-*O*-menthiafoloyl-6-*O*-foliamenthoylmacfadienoside.

The HRESIMS of compound **5** showed a sodiated molecular ion peak at m/z 567.2023 $[M + Na]^+$, consistent with a molecular formula of $C_{25}H_{36}O_{13}$, 166 amu less than that of **4**. Comparison of its NMR spectra (Table 2) with those of **4** showed that **5** differ in the absence of the menthiafoloyl unit linked at C-5. Therefore, **5** was identified as 6-*O*-foliamenthoylmacfadienoside.

Compound **6** was assigned a molecular formula of $C_{24}H_{28}O_{11}$, as deduced from the $[M + Na]^+$ ion at m/z 515.1500 in the positive HRESIMS, as well as from the analysis of its ^{13}C NMR spectroscopic data (Table 2). The NMR spectra (Table 2) showed the presence of an iridoid glycoside moiety superimposable on that of **1** and an aromatic acyl moiety identified as a *trans*-cinnamoyl group [δ 6.63 (H-8'')/117.0 (C-8''), 7.40 (H-3''/H-5'')/128.6 (C-3''/C-5''), 7.40 (H-4'')/130.0 (C-4''), 7.65 (H-2''/H-6'')/128.0 (C-2''/C-6''), 7.81 (H-7'')/145.6 (C-7'')].³ The HMBC experiment supported the location of the ester moiety at C-6, from the correlation peak observed between δ 5.13 (H-6) and 166.6 (C-9''). Therefore, **6** was identified as 6-*O*-*trans*-cinnamoylantirrinoside.

A molecular formula of $C_{24}H_{28}O_{12}$ was assigned to compound **7** as determined by its HRESIMS ($[M + Na]^+$ at m/z 531.1469) and NMR data. In the HRESIMS/MS, a fragment ion at m/z 401.1205 $[M + Na - 130]^+$, was observed, due to the loss of a cinnamoyl residue. Analysis of the NMR data (Table 2) of compound **7** revealed the presence of an iridoid glucoside unit attributable to macfadienoside¹⁴ and a *trans*-cinnamoyl ester moiety. The position of the ester group at C-6' of the glucose moiety was deduced by the HMBC correlation between δ 4.50 (H-6'a_{glc}) and 166.8 ppm (C-9''). Thus, compound **7** was determined as 6'-*O*-*trans*-cinnamoylmacfadienoside.

The HRESIMS of compound **8** exhibited a sodiated molecular ion peak at m/z 727.2787 $[M + Na]^+$, consistent with a molecular formula of $C_{32}H_{48}O_{17}$, as deduced also by its ^{13}C NMR data (Table 3). The positive ESIMS/MS showed peaks at m/z 709 $[M + Na - 18]^+$ and 547 $[M + Na - 18 - 162]^-$, due to the subsequent loss of one water molecule and one hexose residue. The analysis of the ^{13}C

NMR spectrum (Table 3) allowed 16 signals to be attributed to an iridoid glucoside, ten to an ester chain, and six to another sugar residue consisting of a hexose unit. The spectroscopic data of compound **8** (Table 3) showed the presence of a typical conjugated carboxylic enol-ether system of an iridoid with characteristic signals at δ 1.32 (s, Me-10)/24.0 (C-10), 1.70 (m, H₂-7)/39.0 (C-7), 2.15 (dd, $J = 5.5, 4.0$ Hz, H-9)/51.0 (C-9), 2.36, 1.29 (m, H-6a and H-6b)/30.0 (C-6), 3.24 (overlapped signal, H-5)/33.0 (C-5), 5.22 (d, $J = 5.5$ Hz, H-1)/95.6 (C-1), 7.53 (s, H-3)/151.0 (C-3), and of one β -glucopyranose moiety, having an anomeric proton at δ 4.73 (d, $J = 7.7$ Hz). The iridoid portion was thus identified as mussaenosidic acid.¹⁶ The presence of a foliamenthoyl ester moiety linked at C-6 of the glucose unit was also clearly evident from the 1D and 2D spectroscopic data, particularly from the HMBC correlations between δ 4.50/4.30 (H-6'a and H-6'b) and 168.0 (C-1"). Thus, a partial structure of agnucastoside A was recognized.¹⁷ An additional hexose moiety, a fructose unit in a pyranosyl form esterified at C-5, was proposed by means of the 1D and 2D NMR spectra.¹⁸ The carbon chemical shift of the carboxylic function at δ 167.4 (C-11) (171.3 ppm in agnucastoside A)¹⁷ in the iridoid skeleton suggested that the fructopyranose sugar moiety is linked in an ester linkage through C-5. In order to confirm the β -fructopyranose relative configuration, the acetonide derivative **8a** was prepared (Experimental Section). Thus, C-1 and C-2 of the β -fructopyranose unit were shifted from 61.3 and 98.0 ppm to 73.4 and 107.6 ppm, respectively, in the 1,2-*O*-isopropylidene derivative **8a**, in a manner completely in accordance with 1,2-*O*-isopropylidene- β -D-fructopyranose reported in the literature.¹⁹ From these data, the structure of **8** was determined as agnucastoside A 11-(5-*O*- β -D-fructopyranosyl) ester.

Compound **9** showed molecular formula of C₃₂H₄₈O₁₇ by means of HRESIMS (m/z 727.2764 [M + Na]⁺), suggesting it being an isomer of **8**. Analysis of its NMR data (Table 3) and comparison with those of **8** showed that these compounds possess the same iridoid structure, but with a different ester moiety present. Thus, characteristic signals of a menthiafoloyl ester unit were present instead of signals for a foliamenthoyl moiety (δ 1.30 (H-10'')/27.0 (C-10''), 1.71 (H₂-5'')/39.7 (C-5''), 1.86 (H-9'')/12.0 (C-9''), 2.26 (H₂-4'')/24.1 (C-4''), 5.25 (H-8a'')-5.08 (H-8b'')/112.1 (C-8''), 5.94

(H-7'')/145.0 (C-7''), 6.81 (H-3'')/144.0 (C-3''), 72.2 (C-6''), 127.0 (C-2''), and 167.9 (C-1'')). Thus, **9** was elucidated as 6'-*O*-menthiafoloylmussaenosidic acid-11-(5-*O*- β -D-fructopyranosyl) ester.

Compound **10** displayed a molecular formula of C₃₁H₄₀O₁₇ from its HRESIMS (m/z 707.2156 [M + Na]⁺) and NMR data. The ESIMS of **10** showed a sodiated molecular ion peak at m/z 707 [M + Na]⁺ and a fragmentation pattern with peaks at m/z 689 [M + Na - 18]⁺, 545 [M + Na - 162]⁺, and 399 [M + Na - 162 - 146]⁺, corresponding to the subsequent loss of a water molecule, one hexose unit, and one *p*-coumaroyl moiety. Analysis of the NMR data of **10** (Table 3) showed there were close similarities with those of **8**, except for the presence of two coupled signals attributable to *trans*-olefinic protons at δ 6.35 (1H, d, J = 16.0 Hz, H-8''*trans*) and 7.68 (1H, d, J = 16.0 Hz, H-7''*trans*), *cis*-olefinic protons at δ 5.77 (1H, d, J = 12.0 Hz, H-8''*cis*), and 6.87 (1H, d, J = 12.0 Hz, H-7''*cis*), and two *ortho*-coupled A₂B₂ aromatic proton signals at δ 6.78 (2H, d, J = 8.0 Hz, H-3''/H-5''*trans*) and 7.45 (2H, d, J = 8.0 Hz, H-2''/H-6''*trans*), and 6.76 (2H, d, J = 8.0 Hz, H-3''/H-5''*cis*) and 7.66 (2H, d, J = 8.0 Hz, H-2''/H-6''*cis*), instead of signals of the foliamenthoyl ester chain. Thus, compound **10** was identified as an inseparable mixture 1:1 of 6'-*O*-(*trans* and *cis*-*p*-coumaroyl)mussaenosidic acid-11-(5-*O*- β -D-fructopyranosyl) ester. To the best of our knowledge this is the first report of C₁₀ iridoid fructopyranosyl esters.

Compound **11** was assigned a molecular formula of C₂₂H₃₆O₁₃, as determined by its positive HRESIMS data (m/z 531.2021 [M + Na]⁺) and ¹³C NMR spectrum. The positive ESIMS/MS showed peaks at m/z 369 [M + Na - 162]⁺ and 207 [M + Na - 162 - 162]⁻, due to the subsequent loss of two hexose residues. The ¹H and ¹³C NMR spectra (Experimental Section) revealed the presence of two methyl groups attached to double bonds, two methylene groups, two trisubstituted double bonds, and one hydroxymethylene group. A HSQC experiment was used to establish the association of the protons with the corresponding carbons, leading to the characterization of the acyclic monoterpene part of the molecule as 8-hydroxy-2,6-dimethyl-(2*E*,6*E*)-octadienoic acid, or foliamenthic acid.²⁰ Two β -glucopyranosyl units were also evident from the 1D-TOCSY, COSY, and HSQC experiments conducted. The HMBC spectrum indicated the positions of the glucosyl

moieties, showing correlations between δ 5.55 (H-1') and 167.6 (C-1) and δ 4.30 (H-1'') and 65.6 (C-8). Thus, compound **11** was determined as foliamenthic acid 1-*O*- β -D-glucopyranosyl ester 8-*O*- β -D-glucopyranoside.

The molecular formula of compound **12** was determined by HRESIMS to be C₁₆H₂₆O₈ from the sodiated molecular ion peak at *m/z* 369.1594. The ESIMS/MS showed a prominent fragment at *m/z* 207 [M + Na – 162]⁺, due to the loss of a hexose moiety, leading to the inference of the presence of a monoterpene glycoside structure. The monoterpene aglycone moiety was characterized as foliamenthic acid as in **11**²⁰ from the 1D and 2D NMR experiments carried out. Two sets of signals were observed for glucose in the ¹H and ¹³C NMR spectra (Experimental Section), indicating that compound **12** is present as a mutarotational mixture of α - and β -anomers. The HMBC correlation of H-6b_{glc α} and H-6b_{glc β} at δ 4.27 with C-1 at δ 167.8 established the position of the glucose moiety. From these data, the structure of **12** was determined as 6-*O*-foliamenthoyl- α,β -D-glucopyranose.

Compounds (**13-21**) were characterized as 6-*O*-nerol-8-oyl-antirrininose (**13**),³ antirrininose (**14**),¹³ 6-*O*-*trans* and *cis-p*-coumaroyl antirrininose (**15**),¹² 6'-*O*-cinnamoylantirrininose (**16**),³ agnucastin A (**17**),¹⁷ (6*S*)-2*E*-2,6-dimethyl-6-hydroxyocta-2,7-dienoic acid β -glucopyranosyl ester (**18**),²¹ glucosyl 8-hydroxy-2,6-dimethyl-(2*E*,6*E*)-octadienoate (**19**)²⁰, (*S*)-menthiafolinic acid (**20**),²² and foliamenthic acid (**21**)²⁰ by comparison of their NMR and MS literature data.

All of the isolated compounds (**1-21**) were assayed by two *in vivo* models, involving zebrafish embryos and CAMs. The zebrafish is suitable for identification of angiogenesis inhibitors, since development of blood vessels in early embryos is well characterized and easily monitored. A zebrafish endogenous alkaline phosphatase (EAP) assay was used to evaluate the antiangiogenic activity of the isolated compounds from *A. pedatum*. As shown in Figure 1, the results demonstrated that, among the new isolates, compound **9** exhibited the best antiangiogenic activity by reducing significantly (*p* < 0.05) the growth of blood vessels (72.72%) in zebrafish embryos as compared to control used. Weaker effects were observed for the other new isolates in the following order **2** > **3** > **5** > **10** > **7** > **4** > **8** > **1** > **6** > **12** > **11**. In addition, significant antiangiogenic activities were observed

after treatment with the known isolated compounds, **13** (48.33%, $p < 0.01$), **18** (56.98%, $p < 0.01$), **15** (77.38%, $p < 0.05$), **19** (79.82%, $p < 0.05$), **14** (81%, $p < 0.05$). The effects on angiogenesis of *A. pedatum* isolated compounds were compared with that of 2-methoxyestradiol (52%, $p < 0.01$), an endogenous metabolite of 17 β -estradiol having known antiangiogenic and antitumor properties.

In this study, the CAM assay was also performed to explore the antiangiogenic potential of the *A. pedatum* isolates. The CAM, formed on day 4–5 in chicken embryos, shows an extremely dense vascular network. When an angiostatic sample is tested, the vessels become less dense and even disappear. Overall, it is evident that a significant antiangiogenic response was obtained with this experimental model.⁹ The results, as summarized in Figure 2, showed the highest antiangiogenic activities for compounds **9** > **6** > **18** > **13** > **14** > **4**. The effects on angiogenesis, expressed as percentages versus control eggs, were 21.54%, 23.86%, 28.98%, 29.57%, 29.90%, 31.45%, respectively. Retinoic acid, was used as positive standard (45.01%). Images of representative microscopic observations are shown in Figure 3. After six days of incubation, the CAM of control eggs showed the presence of a rich vascular network (Figure 3a). A significant inhibitory effect on capillary formation was observed with retinoic acid (Figure 3b). In the CAMs treated with the more active compounds (**4**, **6**, **9**, **13**, **14**, **18**), the microvasculature appeared less dense (Figures 3c-h). The inhibitory effects on vessel growth were particularly evident after treatment with compound **9** (Figure 3e). Notably, compounds **9**, **13**, and **18** showed a significant activity in both assays. Our results are in accordance with previous reports that have shown the antiangiogenic activity of iridoid derivatives.^{9,23}

EXPERIMENTAL SECTION

General Experimental Procedures. An Atago AP-300 digital polarimeter with a sodium lamp (589 nm) and 1 dm microcell was used to measure optical rotations. NMR experiments were

recorded on Bruker DRX-600 and DRX-500 spectrometers, acquiring the spectra in methanol- d_4 . Standard pulse sequences and phase cycling were used for TOCSY, HSQC, COSY, and HMBC NMR experiments. HRESIMS were obtained in the positive-ion mode on a LTQ Orbitrap XL mass spectrometer (Thermo Fisher Scientific) and Q-TOF premier spectrometer equipped with a nanospray ion source (Waters Milford, MA, USA). ESIMS were obtained from an LCQ Advantage ThermoFinnigan spectrometer (ThermoFinnigan, USA). Column chromatography was performed over Sephadex LH-20. HPCPC chromatography was carried out on a CPC240 Everseiko chromatographer equipped with 3136 cells (240 mL) (Everseiko Co., Japan). HPLC analysis was performed using a Shimadzu LC-8A series pumping system equipped with a Shimadzu RID-10A refractive index detector and Shimadzu injector on a C_{18} μ -Bondapak column (30 cm \times 7.8 mm, 10 μ m Waters, flow rate 2.0 mL/min). TLC separations were carried out using silica gel 60 F₂₅₄ (0.20 mm thickness) plates (Merck) with *n*-BuOH-CH₃COOH-H₂O (60:15:25) as eluent and cerium sulphate as spray reagent. GC analysis was performed using a Dani GC 1000 instrument on a L-CP-Chirasil-Val column (0.32 mm \times 25 m), working with the following temperature program: 100 °C for 1 min, ramp of 5 °C/min up to 180 °C; injector and detector temperature 200 °C; carrier gas N₂ (2 mL/min); detector dual FID; split ratio 1:30; injection 5 μ L.

Plant Material. The aerial parts of *Anarrhinum pedatum* were collected in May 2016 in Djbel El Ouahch, Constantine, Algeria. The plant was identified by Prof. Kamel Kabouche, Université des frères Mentouri-Constantine, Constantine, Algeria, where a voucher specimen (number AP.05.16) has been deposited at the Herbarium of the Department of Chemistry.

Extraction and Isolation. The dried and powdered aerial parts (2 kg) of *A. pedatum* were defatted with *n*-hexane and then extracted successively for 48 h with CHCl₃, CHCl₃-MeOH (9:1), and MeOH, by exhaustive maceration (3 \times 5 L), to give 30.9, 74.9, and 123.1 g of the respective residue. The MeOH extract was partitioned between *n*-BuOH and H₂O to give 55.96 g of a dried *n*-BuOH residue. Part of the *n*-BuOH fraction (10.6 g) was chromatographed on Sephadex LH-20 column chromatography (5 \times 100 cm) using MeOH as eluent at flow rate 1.0 mL/min, collecting

fractions of 10 mL that were analyzed by TLC on silica 60 gel-coated glass with *n*-BuOH-CH₃COOH-H₂O (60:15:25), and grouped into nine major fractions (A-I). Fraction B (523 mg), was subjected to RP-HPLC with MeOH-H₂O (4.5:5.5) to yield agnucastoside A (**17**) (4.8 mg, *t_R* 15 min). Fractions C (2 g) and E (829.5 mg) were separately submitted to HPCPC with CHCl₃-MeOH-H₂O-*i*-PrOH (9:12:8:1), in which the stationary phase consisted of the lower phase (ascending mode, flow rate 3 mL/min), with fractions of 9 and 3 mL collected, respectively. HPCPC fractions C₃ (236 mg) and C₄ (430 mg) were separately purified by RP-HPLC with MeOH-H₂O (3.5:6.5) as eluent to afford compounds **11** (2.0 mg, *t_R* 9 min), **9** (6.6 mg, *t_R* 26 min), and **8** (10.0 mg, *t_R* 30 min) from fraction C₃ and compound **5** (4.1 mg, *t_R* 23 min) from fraction C₄. HPCPC fraction C₇ (97.9 mg) and C₈ (425.6 mg) were subjected by RP-HPLC with MeOH-H₂O (4.5:5.5) to yield compounds **4** (1.9 mg, *t_R* 34 min) and **2** (2.8 mg, *t_R* 39 min) from fraction C₇ and compounds **3** (3.0 mg, *t_R* 42 min) and **1** (11 mg, *t_R* 47 min) from fraction C₈. HPCPC fractions E₂ (90.5 mg), E₅ (43.9 mg), and E₆ (63.7 mg) were chromatographed by RP-HPLC with MeOH-H₂O (3:7) to obtain **14** (1.3 mg, *t_R* 6 min) and compound **10** (7.4 mg, *t_R* 33 min) from fraction E₂, **18** (2.9 mg, *t_R* 16 min), **19** (2.1 mg, *t_R* 18 min), and compound **12** (2.0 mg, *t_R* 24 min) from fraction E₅, and compounds **12** (4.5 mg, *t_R* 24 min) and **7** (2.9 mg, *t_R* 41 min) from fraction E₆. HPCPC fraction E₇ (59 mg) after separation with RP-HPLC with MeOH-H₂O (3.5:6.5) yielded **20** (3.6 mg, *t_R* 25 min), **21** (8.3 mg, *t_R* 27 min), **16** (2.3 mg, *t_R* 54 min), and compound **6** (3.8 mg, *t_R* 62 min). Fraction D (410.6 mg) was purified by RP-HPLC with MeOH-H₂O (3.5:6.5) as eluent to give **18** (2.9 mg, *t_R* 12 min), **19** (1.8 mg, *t_R* 14 min), and **13** (2.0 mg, *t_R* 45 min). Fraction F (252.9 mg) was chromatographed over by RP-HPLC with MeOH-H₂O (3:7) as eluent to obtain **15** (1.5 mg, *t_R* 45 min) from fraction F.

Compound (1): amorphous powder; $[\alpha]_D^{25}$ -70 (*c* 0.1, MeOH); ¹H and ¹³C NMR, see Table 1; ESIMS *m/z* 693 [M - H]⁻, 649 [M - H - 44]⁻, 717 [M + Na]⁺, 699 [M + Na - 18]⁺, 551 [M + Na - 166]⁺; HRESIMS *m/z* 717.3090 [M + Na]⁺, 695.3278 [M + H]⁺ (calcd for C₃₅H₅₀O₁₄Na 717.3098).

Compound (2): amorphous powder; $[\alpha]_{\text{D}}^{25} +41$ (*c* 0.1, MeOH); ^1H and ^{13}C NMR, see Table 1; ESIMS m/z 709 $[\text{M} - \text{H}]^-$, 733 $[\text{M} + \text{Na}]^+$; HRESIMS m/z 711.3229 $[\text{M} + \text{H}]^+$ (calcd for $\text{C}_{35}\text{H}_{51}\text{O}_{15}$ 711.3228).

Compound (3): amorphous powder; $[\alpha]_{\text{D}}^{25} -45$ (*c* 0.1, MeOH); ^1H and ^{13}C NMR, see Table 1; HRESIMS m/z 717.3083 $[\text{M} + \text{Na}]^+$, 551.2084 $[\text{M} + \text{Na} - 166]^+$, 533.1976 $[\text{M} + \text{Na} - 184]^+$, 349.0883 $[\text{M} + \text{Na} - 184 - 184]^+$ (calcd for $\text{C}_{35}\text{H}_{50}\text{O}_{14}\text{Na}$ 717.3098).

Compound (4): amorphous powder; $[\alpha]_{\text{D}}^{25} +70$ (*c* 0.1, MeOH); ^1H and ^{13}C NMR, see Table 1; HRESIMS m/z 733.3040 $[\text{M} + \text{Na}]^+$, 549.1961 $[\text{M} + \text{Na} - 184]^+$ (calcd for $\text{C}_{35}\text{H}_{50}\text{O}_{15}\text{Na}$ 733.3047).

Compound (5): amorphous powder; $[\alpha]_{\text{D}}^{25} +25$ (*c* 0.1, MeOH); ^1H and ^{13}C NMR, see Table 2; HRESIMS m/z 567.2023 $[\text{M} + \text{Na}]^+$, 549.1922 $[\text{M} + \text{Na} - 18]^+$, 405.1504 $[\text{M} + \text{Na} - 162]^+$, 387.1401 $[\text{M} + \text{Na} - 162 - 18]^+$, 383.0937 $[\text{M} + \text{Na} - 184]^+$ (calcd for $\text{C}_{25}\text{H}_{36}\text{O}_{13}\text{Na}$ 567.2054).

Compound (6): amorphous powder; $[\alpha]_{\text{D}}^{25} -120$ (*c* 0.1, MeOH); ^1H and ^{13}C NMR, see Table 2; ESIMS m/z 515 $[\text{M} + \text{Na}]^+$; HRESIMS m/z 515.1500 $[\text{M} + \text{Na}]^+$, 497.1386 $[\text{M} + \text{Na} - 18]^+$, 353.0975 $[\text{M} + \text{Na} - 162]^+$ (calcd for $\text{C}_{24}\text{H}_{28}\text{O}_{11}\text{Na}$ 515.1529).

Compound (7): amorphous powder; $[\alpha]_{\text{D}}^{25} -66$ (*c* 0.1, MeOH); ^1H and ^{13}C NMR, see Table 2; ESIMS m/z 531 $[\text{M} + \text{Na}]^+$, 513 $[\text{M} + \text{Na} - 18]^+$, 507 $[\text{M} - \text{H}]^-$, 489 $[\text{M} - \text{H} - 18]^-$; HRESIMS m/z 531.1469 $[\text{M} + \text{Na}]^+$, 513.1355 $[\text{M} + \text{Na} - 18]^+$, 401.1205 $[\text{M} + \text{Na} - 130]^+$ (calcd for $\text{C}_{24}\text{H}_{28}\text{O}_{12}\text{Na}$ 531.1478).

Compound (8): amorphous powder; $[\alpha]_{\text{D}}^{25} -168$ (*c* 0.1, MeOH); ^1H and ^{13}C NMR, see Table 3; ESIMS m/z 727 $[\text{M} + \text{Na}]^+$, 709 $[\text{M} + \text{Na} - 18]^+$, 547 $[\text{M} + \text{Na} - 18 - 162]^+$; HRESIMS m/z 727.2787 $[\text{M} + \text{Na}]^+$, 709.2658 $[\text{M} + \text{Na} - 18]^+$, 547.2139 $[\text{M} + \text{Na} - 18 - 162]^+$ (calcd for $\text{C}_{32}\text{H}_{48}\text{O}_{17}\text{Na}$ 727.2789).

Compound (9): amorphous powder; $[\alpha]_{\text{D}}^{25} -70$ (c 0.1, MeOH); ^1H and ^{13}C NMR, see Table 3; ESIMS m/z 727 $[\text{M} + \text{Na}]^+$, 565 $[\text{M} + \text{Na} - 162]^+$, 703 $[\text{M} - \text{H}]^-$, 541 $[\text{M} - \text{H} - 162]^-$; HRESIMS m/z 727.2764 $[\text{M} + \text{Na}]^+$, 565.2240 $[\text{M} + \text{Na} - 162]^+$ (calcd for $\text{C}_{32}\text{H}_{48}\text{O}_{17}\text{Na}$ 727.2789).

Compound (10): amorphous powder; $[\alpha]_{\text{D}}^{25} -115$ (c 0.1, MeOH); ^1H and ^{13}C NMR, see Table 3; ESIMS m/z 707 $[\text{M} + \text{Na}]^+$, 689 $[\text{M} + \text{Na} - 18]^+$, 545 $[\text{M} + \text{Na} - 162]^+$, 527 $[\text{M} + \text{Na} - 18 - 162]^+$, 399 $[\text{M} + \text{Na} - 162 - 146]^+$, 683 $[\text{M} - \text{H}]^-$; HRESIMS m/z 707.2156 $[\text{M} + \text{Na}]^+$, 689.2048 $[\text{M} + \text{Na} - 18]^+$, 527.1515 $[\text{M} + \text{Na} - 18 - 162]^+$, 381.1153 $[\text{M} + \text{Na} - 18 - 162 - 146]^+$ (calcd for $\text{C}_{31}\text{H}_{40}\text{O}_{17}\text{Na}$ 707.2163).

Compound (11): amorphous powder; $[\alpha]_{\text{D}}^{25} +34$ (c 0.1, MeOH); ^1H NMR data (CD_3OD , 500 MHz) δ 1.81 (3H, s, Me-10), 1.88 (3H, s, Me-9), 2.32 (2H, m, H₂-5), 2.37 (2H, m, H₂-4), 3.20 (1H, br t, $J = 9.0$ Hz, H-2_{glcII}), 3.29 (2H, overlapped, H-4_{glcII} and H-5_{glcII}), 3.39 (1H, overlapped, H-5_{glcI}), 3.40 (1H, overlapped, H-4_{glcI} and H-3_{glcII}), 3.42 (1H, overlapped, H-2_{glcI}), 3.43 (1H, overlapped, H-3_{glcI}), 3.70 (2H, dd, $J = 12.0, 5.0$ Hz, H-6b_{glcI} and H-6b_{glcII}), 3.87 (2H, dd, $J = 12.0, 2.5$ Hz, H-6a_{glcI} and H-6b_{glcII}), 4.24 (1H, dd, $J = 11.0, 3.0$ Hz, H-8b), 4.36 (1H, dd, $J = 11.0, 5.0$ Hz, H-8a), 5.48 (1H, br d, $J = 6.6$ Hz, H-7), 5.55 (1H, d, $J = 7.5$ Hz, H-1_{glcI}), 6.93 (1H, br t, $J = 6.6$ Hz, H-3); ^{13}C NMR data (CD_3OD , 125 MHz) δ 12.0 (C-9), 23.0 (C-10), 27.0 (C-4), 30.2 (C-5), 62.3 (C-6_{glcI} and C-6_{glcII}), 65.6 (C-8), 70.8 (C-4_{glcI}), 71.3 (C-4_{glcII}), 73.6 (C-2_{glcI}), 74.7 (C-2_{glcII}), 77.0 (C-3_{glcI} and C-3_{glcII}), 77.5 (C-5_{glcII}), 78.1 (C-5_{glcI}), 95.0 (C-1_{glcI}), 102.0 (C-1_{glcII}), 123.0 (C-7), 127.7 (C-2), 139.5 (C-6), 143.4 (C-3), 167.6 (C-1); ESIMS m/z 531 $[\text{M} + \text{Na}]^+$, 369 $[\text{M} + \text{Na} - 162]^+$, 207 $[\text{M} + \text{Na} - 162 - 162]^+$, 507 $[\text{M} - \text{H}]^-$, 345 $[\text{M} - \text{H} - 162]^-$, 183 $[\text{M} - \text{H} - 162 - 162]^-$; HRESIMS m/z 531.2021 $[\text{M} + \text{Na}]^+$, 369.1502 $[\text{M} + \text{Na} - 162]^+$ (calcd for $\text{C}_{22}\text{H}_{36}\text{O}_{13}\text{Na}$ 531.2054).

Compound (12): amorphous powder; $[\alpha]_{\text{D}}^{25} +61$ (c 0.1, MeOH); ^1H NMR data (CD_3OD , 600 MHz) δ 1.77 (3H, s, Me-10), 1.81 (3H, s, Me-9), 2.23 (2H, m, H₂-5), 2.40 (2H, m, H₂-4), 3.16 (1H, br t, $J = 8.0$ Hz, H-2_{glc α}), 3.37 (3H, overlapped, H-2_{glc β} , H-3_{glc β} , and H-4_{glc β}), 3.38 (1H, overlapped, H-5_{glc α}), 3.52 (1H, m, H-5_{glc β}), 3.69 (1H, t, $J = 9.3$ Hz, H-3_{glc α}), 4.00 (1H, m, H-4_{glc α}), 4.27 (2H, overlapped,

H-6b_{glc α} and H-6b_{glc β}), 4.39 (1H, dd, $J = 12.0, 2.0$ Hz, H-6a_{glc α}), 4.46 (1H, dd, $J = 12.0, 2.0$ Hz, H-6a_{glc β}), 4.50 (1H, d, $J = 8.0$ Hz, H-1_{glc β}), 4.08 (2H, d, $J = 7.2$ Hz, H₂-8), 5.10 (1H, d, $J = 3.5$ Hz, H-1_{glc α}), 5.42 (1H, br d, $J = 7.0$ Hz, H-7), 6.78 (1H, br t, $J = 7.6$ Hz, H-3); ¹³C NMR data (CD₃OD, 150 MHz) δ 12.0 (C-9), 23.2 (C-10), 27.4 (C-4), 31.8 (C-5), 64.1 (C-6_{glc α}), 64.8 (C-6_{glc β}), 58.4 (C-8), 70.1 (C-4_{glc β}), 71.0 (C-4_{glc α}), 72.0 (C-5_{glc α}), 74.0 (C-2_{glc α}), 74.1 (C-3_{glc α}), 75.1 (C-5_{glc β}), 76.0 (C-2_{glc β}), 77.5 (C-3_{glc β}), 92.0 (C-1_{glc α}), 97.3 (C-1_{glc β}), 126.6 (C-7), 128.3 (C-2), 136.5 (C-6), 143.6 (C-3), 167.8 (C-1); ESIMS m/z 369 [M + Na]⁺, 351 [M + Na - 18]⁺, 207 [M + Na - 162]⁺; HRESIMS m/z 369.1594 [M + Na]⁺, 207.0869 [M + Na - 162]⁺ (calcd for C₁₆H₂₆O₈Na 369.1525).

Acid Hydrolysis of Compounds 1-12. Acid hydrolysis of compounds **1-12** was carried out as reported in a previous study.²⁴ D-Glucose and D-fructose were identified as the sugar moiety in each case by comparison with the retention times of authentic samples.

Preparation of Acetonide Derivative. A suspension of compound **8** (6.0 mg) in THF (2.0 mL) was treated with 2,2-dimethoxypropane (1 mL), followed by a catalytic amount of anhydrous *p*-TsOH at 25 °C. After 1 h of stirring, a few drops of Et₃N were added, and the mixture was concentrated under a vacuum. The residue was partitioned between CHCl₃ and a saturated solution of NaHCO₃ and the chloroform part was concentrated under a vacuum, affording the acetonide **8a**.

Zebrafish Embryo Generation and Staging, Treatment Protocol. Zebrafish (*Danio rerio*) embryos were obtained from wild type fish bought from a local pet store and maintained in flow through aquaria at 28.5 °C on a 14/10 h (light/dark) photoperiod. Embryos were generated by natural mating as described by Kimmel et al.²⁵ and they were cultured in water at 28.5 °C. All experiments were performed in compliance with the European Directive 2010/63/EU and the ethical guidelines described in the “National Institutes of Health Guide for Care and Use of Laboratory Animals”. Then, healthy and regular embryos were selected at 24 h post fertilization (hpf), manually dechorionated with forceps, distributed in 96 single well microplates (one embryo per well) and finally incubated with 100 μ L of embryo water containing isolated compounds (2 μ M) or 2-methoxyestradiol (ME, 2 μ M), employed as a standard antiangiogenic substance. DMSO (0.2% v/

v) was used as a vehicle for those treatments. Control group received only DMSO (0.2% v/v). All treated embryos (10 for each group) were incubated from 24 hpf to 72 hpf (total 48 h of exposure).

Quantitative Determination of Endogenous Alkaline Phosphatase (EAP) Activity.

Quantitative determination of EAP activity was performed as described by Germanò et al.²⁶ Zebrafish treated embryos at 72 hpf were dehydrated with increasing concentrations of ethanol, then they were washed three times with diethanolamine buffer (1 M, pH 9.8), and incubated with the substrate containing 0.5 mg/mL *p*-nitrophenyl phosphate disodium salt (Sigma Aldrich) for 30 min at room temperature. NaOH (2 M) was added to stop the reaction. The optical density (OD) of soluble end product was measured at 405 nm using a microplate reader (Mutiskan GO, Thermo Scientific). Vessel growth was expressed as a percentage of formation respect to control embryos which were considered 100%. Each assay was repeated at least three times. The significance of the differences was assessed on the basis of the *t*-test, considering the differences for $p < 0.05$ and $p < 0.01$, and finally calculated versus control embryos.

Chorioallantoic Membrane Assay (CAM). CAM assay was performed following the method of Certo et al.²⁷ Fertilized chicken eggs were incubated at 37 °C. The eggs were positioned horizontally and rotated for several times. After 4 days of incubation, a window (1 cm²) was carefully created on the broad side of the egg to assess the extent of embryonic blood vessels. The development of the embryos was checked by a visual inspection. Malformed or dead embryos were excluded. Then, isolated compounds were tested at 2 μM (100 μL/egg). Ten eggs were used for each group. DMSO (0.2% v/v) in Tris buffer (pH 7.4) was used as a vehicle for those treatments. Retinoic acid (3 μM) was used as positive control. After treatment, the eggs were reincubated for other two days. At the end of incubation, each egg was observed under a stereomicroscope (SMZ-171 Series, Motic) to visualize the microvasculature of the CAM. The images of each CAM were acquired by a digital camera (Moticam® 5 plus) for quantification of the effects on angiogenesis in a standardized area using an open source Java image-processing program. The angiogenic activity was finally expressed as percentage respect to control which was considered 100%. Each

experiment was repeated three times. The significance of the differences was assessed on the basis of the *t*-test, considering the differences for $p < 0.05$ and $p < 0.01$, and finally calculated versus control eggs.

ASSOCIATED CONTENT

Supporting Information. HRESIMS and NMR spectra of compounds **1-12**. This material is available via the Internet at <http://pubs.acs.org>.

AUTHOR INFORMATION

Corresponding Author

*Tel: +39-050-2219688. Fax: +39-050-2220680. E-mail: alessandra.braca@unipi.it

ORCID[®]

Maria Paola Germanò: 0000-0002-4300-5413

Nunziatina De Tommasi: 0000-0003-1707-4156

Felicia D'Andrea: 0000-0003-1517-4911

Alessandra Braca: 0000-0002-9838-0448

Marinella De Leo: 0000-0002-5544-8457

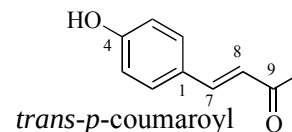
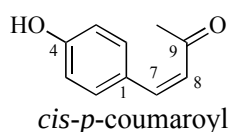
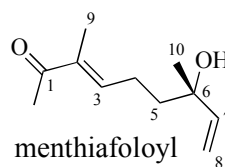
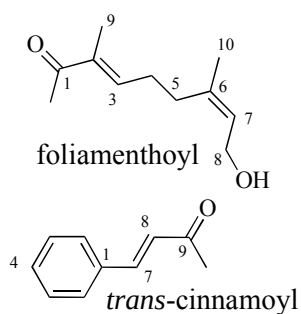
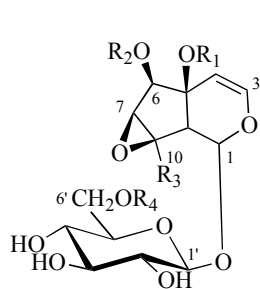
Notes

The authors declare no competing financial interest.

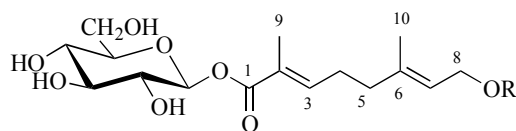
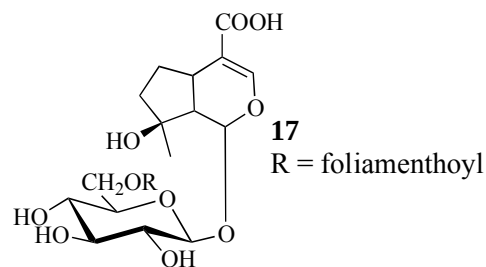
REFERENCES

- (1) Tutin, T. G.; Heywood, V. H.; Burges N. A.; Valentine D. H.; Walters S. M.; Webb D. A. *Flora Europaea*; Cambridge University Press: Cambridge, U. K., 1972; Vol. III, pp 220–221.
- (2) Dobignard, A.; Chatelain C. *Index Synonymique de la Flore d'Afrique du Nord*; Conservatoire et Jardin Botaniques: Geneva, 2013; Vol. 5, p 66.
- (3) Dawidar, A. M.; Esmirly, S. T.; Al-hajar, A. S. M.; Jakupovic, J.; Abdel-mogib, M. *Phytochemistry* **1989**, *28*, 3227–3229.
- (4) Salah El Dine, R.; Abdel Monem, A. R.; El-Halawany, A. M.; Hattori, M; Abdel-Sattar, E. *J. Nat. Prod.* **2011**, *74*, 943–948.
- (5) Habtemariam, S. *Molecules* **2018**, *23*, 117/1-117/23.
- (6) Avasthi, P.; Gupta, N.; Sapra, S.; Dhar, K. L. *Int. J. Pharm. Sci. Lett.* **2013**, *3*, 183-189.
- (7) Beladjila, K. A.; Cotugno, R.; Berrehal, D.; Kabouche, Z.; De Tommasi, N.; Braca, A.; De Leo, M. *Nat. Prod. Res.* **2018**, *32*, 2025–2030.
- (8) Beladjila, K. A.; Berrehal, D.; De Tommasi, N.; Granchi, C.; Bononi, G.; Braca, A.; De Leo, M. *Planta Med.* **2018**, *84*, 710–715.
- (9) Muñoz Camero, C.; Germanò, M. P.; Rapisarda, A.; D'Angelo, V.; Amira, S.; Benchikh, F.; Braca, A.; De Leo, M. *Rev. Bras. Farmacogn.* **2018**, *28*, 374–377.
- (10) Quezel, P; Santa, S. *Nouvelle Flore de l'Algérie et Des Régions Désertiques Méridionales*; C.N.R.S.: Paris, 1963; p 846.
- (11) Hamel, T.; Seridi, R.; de Bélair, G.; Slimani, A.; Babali, B. *Rev. Sci. Technol. Synthèse* **2013**, *26*, 65–74.
- (12) Ilieva, E. I.; Handjieva, N. V., Popov, S. S. *Phytochemistry* **1992**, *31*, 1040–1041.
- (13) Ercil, D.; Sakar, M. K.; Del Olmo, E.; San Feliciano, A. *Turk. J. Chem.* **2004**, *28*; 133–139.
- (14) Bianco, A.; Guiso, M.; Iavarone, C.; Trogolo, C. *Gazz. Chim. Ital.* **1974**, *104*, 731–738.
- (15) Handjieva, N.; Tersieva, L.; Popov, S.; Evstatieva, L. *Phytochemistry* **1995**, *39*, 925–927.

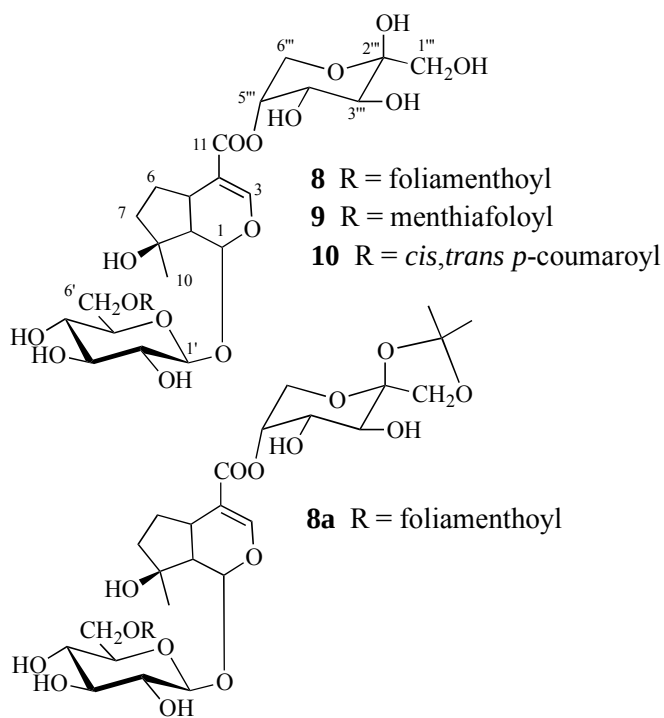
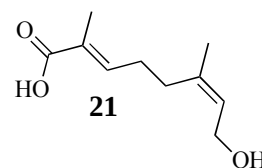
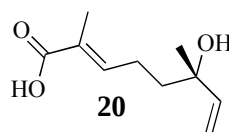
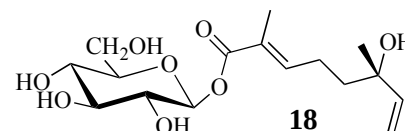
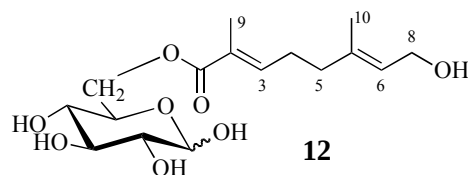
- (16) Damtoft, S.; Hansen, S. B.; Jacobsen, B.; Jensen, S. R.; Nielsen, B. J. *Phytochemistry* **1984**, *23*, 2387–2389.
- (17) Kuruüzüm-Uz, A.; Ströch, K.; Demirezer, L. Ö.; Zeeck, A. *Phytochemistry* **2003**, *63*, 956–964.
- (18) Zhang, C. Z.; Xu, X. Z.; Li, C. *Phytochemistry* **1996**, *41*, 975–976.
- (19) Racine, E.; Burchak, O. N.; Py, S. *Eur. J. Org. Chem.* **2016**, 4003–4012.
- (20) Iwagawa, T.; Asai, H.; Hase, T.; Sako, S.; Su, R.; Hagiwara, N.; Kim, M. *Phytochemistry* **1990**, *29*, 1913–1916.
- (21) Takeda, Y.; Takechi, A.; Masuda, T.; Otsuka, H. *Planta Med.* **1998**, *64*, 78–79.
- (22) Arslanian, R. L.; Anderson, T.; Stermitz, F. R. *J. Nat. Prod.* **1990**, *53*, 1485–1489.
- (23) Koo, H. J.; Lee, S.; Shin, K. H.; Kim, B. C.; Lim, C. J.; Park, E. H. *Planta Med.* **2004**, *70*, 467–469.
- (24) Milella, L.; Milazzo, S.; De Leo, M.; Vera Saltos, M. B.; Immacolata, F.; Tuccinardi, T.; Lapillo, M.; De Tommasi, N.; Braca, A. *J. Nat. Prod.* **2016**, *79*, 2104–2112.
- (25) Kimmel, C. B.; Ballard, W. W.; Kimmel, S. R.; Wullmann, B.; Schilling, T. F. *Develop. Dynam.* **1995**, *203*, 253–310.
- (26) Germanò, M. P.; Certo, G.; D'Angelo, V.; Sanogo, R.; Malafronte, N.; De Tommasi, N.; Rapisarda, A. *Nat. Prod. Res.* **2015**, *29*, 1551–1556.
- (27) Certo, G.; Costa, R.; D'Angelo, V.; Russo, M.; Albergamo, A.; Dugo, G.; Germanò, M. P. *Nat. Prod. Res.* **2017**, *31*, 2850–2856.



- 1 R₁ = R₂ = foliamenthoyl R₃ = CH₃ R₄ = H
 2 R₁ = R₂ = foliamenthoyl R₃ = CH₂OH R₄ = H
 3 R₁ = menthiafoloyl R₂ = foliamenthoyl R₃ = CH₃ R₄ = H
 4 R₁ = menthiafoloyl R₂ = foliamenthoyl R₃ = CH₂OH R₄ = H
 5 R₁ = R₄ = H R₂ = foliamenthoyl R₃ = CH₂OH
 6 R₁ = R₄ = H R₂ = *trans*-cinnamoyl R₃ = CH₃
 7 R₁ = R₂ = H R₃ = CH₂OH R₄ = *trans*-cinnamoyl
 13 R₁ = R₄ = H R₂ = foliamenthoyl R₃ = CH₃
 14 R₁ = R₂ = R₄ = H R₃ = CH₃
 15 R₁ = R₄ = H R₂ = *cis, trans p*-coumaroyl R₃ = CH₃
 16 R₁ = R₂ = H R₃ = CH₃ R₄ = *trans*-cinnamoyl



19 R = H



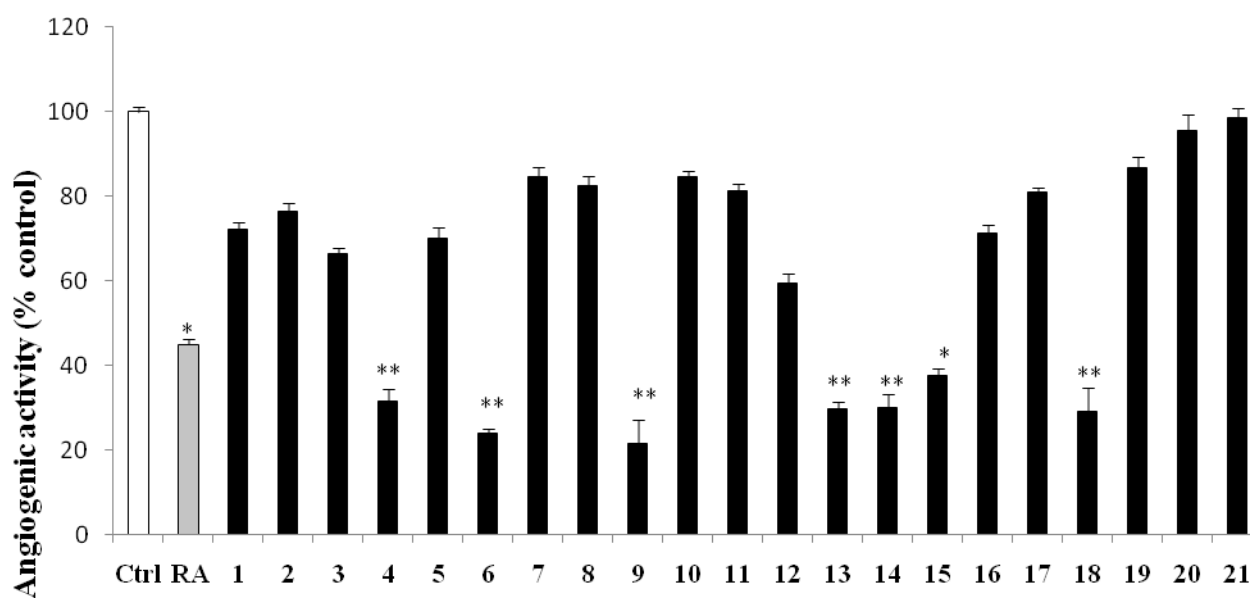


Figure 2. Angiogenic activity (% vs. control) of compounds **1-21** ($2 \mu\text{M}$) in the CAM assay. RA = retinoic acid ($3 \mu\text{M}$). * $p < 0.05$ and ** $p < 0.01$ vs control: Student's t -test.

Figure 3. Antiangiogenic activity of *A. pedatum* compounds (2 μ M) in the CAM assay

a = control, b = retinoic acid (3 μ M), c = **4**, d = **6**, e = **9**, f = **13**, g = **14**, and h = **18**. The images of CAMs were captured using a stereomicroscope (SMZ-171 Series, Motic) equipped with a digital camera (Moticam® 5 plus).

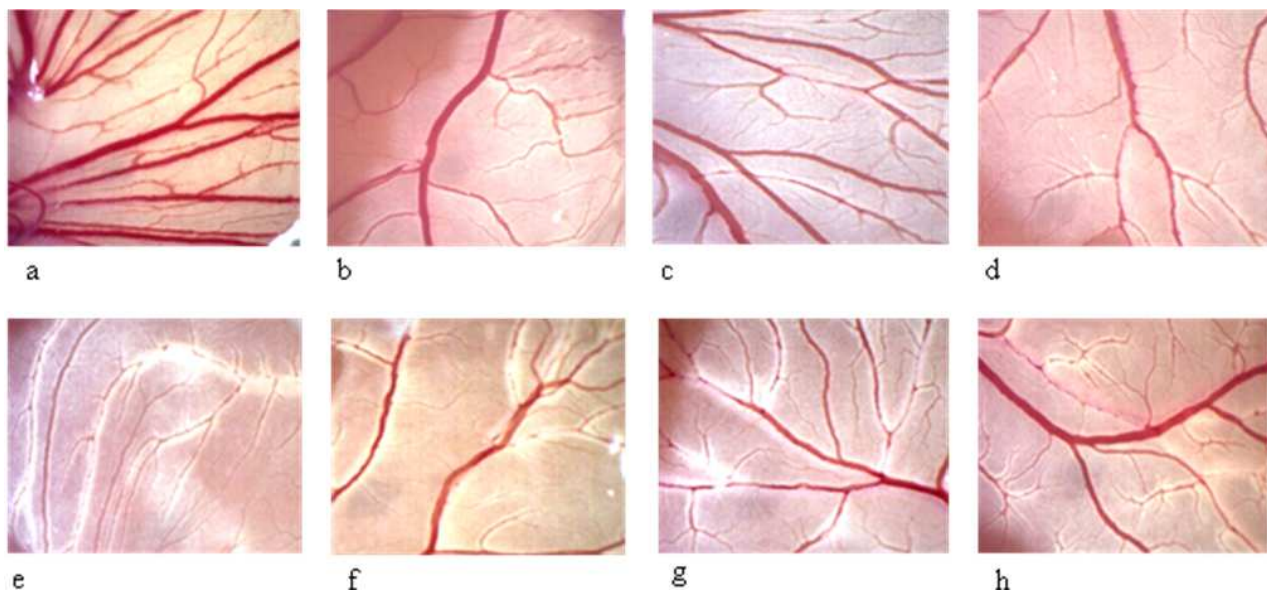


Table 1. ^1H and ^{13}C NMR Data of Compounds **1-4**^a

position	1		2		3		4	
	δ_{H}	δ_{C}	δ_{H}	δ_{C}	δ_{H}	δ_{C}	δ_{H}	δ_{C}
1	5.82 d (2.2)	93.5	5.98 d (2.2)	92.3	5.81 d (2.0)	93.5	5.96d (2.7)	92.8
3	6.59 d (6.5)	145.6	6.58 d (6.5)	145.4	6.58 d (6.5)	145.6	6.56 d (6.7)	145.5
4	5.48 d (6.5)	102.4	5.49 d (6.5)	102.4	5.49 d (6.5)	102.4	5.47 d (6.7)	102.6
5		80.3		80.5		79.0		80.6
6	5.15 d (2.0)	76.5	5.19 d (2.0)	76.2	5.15 d (2.2)	76.3	5.17 d (2.0)	76.2
7	3.63 d (2.0)	64.0	3.78 d (2.0)	60.9	3.63 d (2.4)	64.3	3.71 d (2.0)	61.4
8		64.6		66.6		64.0		66.0
9	2.86 br s	49.4	3.01 br s	49.0	2.88 br s	50.1	3.02 br s	48.8
10a	1.49 s	16.0	4.16 d (13.0)	61.1	1.50 s	16.1	4.14 d (13.0)	61.0
10b			3.56 d (13.0)				3.56 d (13.0)	
glc-1'	4.68 d (7.8)	100.0	4.70 d (8.0)	100.4	4.71 d (7.8)	100.5	4.68 d (7.7)	100.4
2'	3.23 br t (9.0)	74.4	3.22 br t (9.0)	73.8	3.23 br t (9.0)	74.6	3.22 br t (9.5)	74.0
3'	3.37 t (9.5)	77.7	3.36 t (9.5)	77.6	3.37 t (9.5)	77.9	3.35 ^b	77.6
4'	3.31 t (9.5)	70.9	3.35 t (9.5)	71.2	3.32 t (9.5)	71.2	3.34 ^b	71.1
5'	3.40 m	77.8	3.41 m	77.4	3.40 m	77.9	3.38 m	77.4
6'a	3.97 dd (12.0, 3.0)	62.4	3.94 dd (12.0, 3.0)	62.0	3.98 dd (12.0, 2.5)	62.4	3.94 dd (12.0, 2.0)	62.7
6'b	3.71 dd (12.0, 5.5)		3.73 dd (12.0, 5.0)		3.73 dd (12.0, 5.0)		3.71 dd (12.0, 4.5)	
1''		167.3		167.1		166.0		166.0
2''		128.3		128.9		125.1		127.2
3''	6.78 br t (6.9)	142.6	6.79 br t (6.9)	143.1	6.71 br t (7.3)	144.3	6.71 br t (7.0)	144.4
H ₂ -4''	2.31 ^b m	27.5	2.33 ^b m	26.4	2.23 m	24.1	2.23 m	24.0
H ₂ -5''	2.19 ^b m	31.1	2.22 ^b m	30.8	1.59 t (8.2)	41.5	1.57 t (8.2)	41.5
6''		137.8		138.6		71.8		72.1
7''	5.43 br d (7.7) ^b	126.0	5.44 br d (7.7) ^b	125.2	5.93 dd (16.9, 12.0)	145.5	5.93 dd (17.0, 11.0)	145.0
8''a	4.09 ^b	58.6	4.06 ^b	58.6	5.27 br d (17.1)	112.1	5.25 br d (17.0)	112.1
8''b	4.09 ^b		4.06 ^b		5.07 br d (11.4)		5.07 br d (11.0)	
9''	1.80 ^b s	13.0	1.81 s	12.5	1.80 ^b s	12.0 ^b	1.80 s	12.0
10''	1.79 ^b s	23.0	1.78 s	22.8	1.29 s	27.4	1.28 s	27.4
1'''		167.8		167.8		165.7		166.0
2'''		128.3		128.4		127.0		128.5
3'''	6.69 br t (6.9)	143.0	6.71 br t (6.9)	143.4	6.78 br t (7.6)	143.1	6.77 br t (7.3)	143.3
H ₂ -4'''	2.31 ^b m	27.5	2.33 ^b m	26.4	2.34 m ^b	27.8	2.33 m ^b	27.8
H ₂ -5'''	2.19 ^b m	31.0	2.22 ^b m	30.8	2.25 ^b	31.4	2.23 ^b	31.3
6'''		137.8		138.6		136.2		137.5
7'''	5.43 br d (7.7) ^b	126.0	5.44 br d (7.7) ^b	125.2	5.46 br d (7.0)	126.2	5.46 br d (6.5)	126.2
H ₂ -8'''	4.09 ^b	58.6	4.06 ^b	58.6	4.11 d (6.7)	59.0	4.10 d (6.5)	58.8
9'''	1.80 ^b s	12.0	1.81 s	11.6	1.80 ^b s	12.0 ^b	1.79 s	12.0
10'''	1.79 ^b s	23.0	1.78 s	22.8	1.81 s	23.0	1.78 s	23.2

^aSpectra were run in methanol-*d*₄ at 600 MHz (¹H) and 150 MHz (¹³C) for **1** and **2**, at 500 MHz (¹H) and 125 MHz (¹³C) for **3** and **4**. *J* values are in parentheses and reported in Hz; chemical shifts are given in ppm; assignments were confirmed by COSY, 1D-TOCSY, HSQC, and HMBC experiments. ^bOverlapped signal.

Table 2. ^1H and ^{13}C NMR Data of Compounds **5-7**^a

position	5		6		7	
	δ_{H}	δ_{C}	δ_{H}	δ_{C}	δ_{H}	δ_{C}
1	5.55 d (7.5)	94.3	5.57 d (6.4)	93.3	5.24 d (8.5)	95.0
3	6.42 d (6.0)	142.6	6.43 d (6.5)	142.0	6.39 d (6.2)	142.0
4	4.97 d (6.2)	107.3	4.97 d (6.5)	106.0	4.92 d (6.2)	107.0
5		73.5		73.3		73.0
6	5.10 br s	79.2	5.13 d (2.0)	77.2	3.96 d (1.7)	77.6
7	3.72 br d (2.0)	58.0	3.58 d (2.0)	61.6	3.57 ^b	62.2
8		65.0		63.1		65.0
9	2.63 d (7.5)	51.1	2.50 d (6.4)	52.0	2.57 d (8.5)	50.3
10a	4.15 d (13.5)	60.8	1.51 s	17.0	4.11 d (12.8)	60.6
10b	3.71 d (13.5)				3.62 d (12.8)	
glc-1'	4.72 d (8.0)	99.3	4.68 d (8.0)	98.4	4.71 d (8.0)	99.0
2'	3.25 br t (9.0)	74.3	3.25 ^b	73.4	3.30 ^b	74.0
3'	3.34 t (9.0)	78.2	3.35 t (9.5)	78.3	3.44 t (9.5)	77.0
4'	3.28 t (9.5)	71.3	3.26 ^b	70.4	3.43 t (9.5)	71.1
5'	3.44 m	77.3	3.43 m	76.4	3.57 ^b	75.0
6'a	3.93 dd (12.0, 3.0)	62.4	3.98 dd (12.0, 2.0)	62.8	4.50 dd (12.0, 2.3)	63.6
6'b	3.66 dd (12.0, 5.0)		3.60 dd (12.0, 6.0)		4.36 dd (12.0, 5.5)	
1''		167.8		134.3		134.0
2''		128.1	7.65 dd (7.5, 2.8)	128.0	7.64 dd (7.5, 3.0)	128.2
3''	6.94 br t (7.4)	143.9	7.40 ^b	128.6	7.42 ^b	130.0
4''a	2.36 m ^b	28.0	7.40 ^b	130.0	7.42 ^b	131.2
4''b	2.36 m ^b					
5''	2.26 br t (7.6) ^b	31.1	7.40 ^b	128.6	7.42 ^b	130.0
6''		138.1	7.65 dd (7.5, 2.8)	128.0	7.64 dd (7.5, 3.0)	128.2
7''	5.43 br d (6.4)	126.2	7.81 d (16.5)	145.6	7.70 d (16.0)	146.4
8''	4.10 d (6.4) ^b	58.8	6.63 d (16.5)	117.0	6.59 d (16.0)	117.5
9''	1.90 s	12.1		166.6		166.8
10''	1.78 s	23.1				

^aSpectra were run in methanol-*d*₄ at 500 MHz (^1H) and 125 MHz (^{13}C) for **5** and **6**, at 600 MHz (^1H) and 150 MHz (^{13}C) for **7**. *J* values are in parentheses and reported in Hz; chemical shifts are given in ppm; assignments were confirmed by COSY, 1D-TOCSY, HSQC, and HMBC experiments. ^bOverlapped signal.

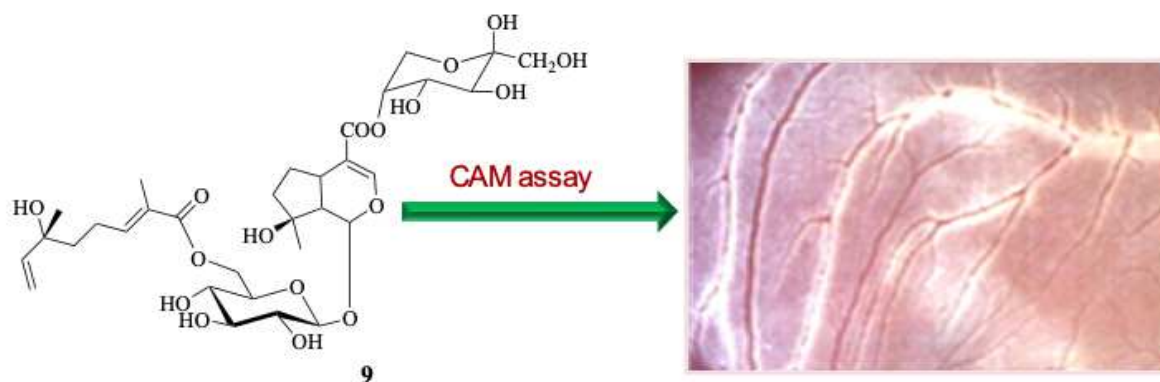
Table 3. ¹H and ¹³C NMR Data of Compounds **8-10**^a

position	8		9		10	
	δ_{H}	δ_{C}	δ_{H}	δ_{C}	δ_{H}	δ_{C}
1	5.22 d (5.5)	95.6	5.25 ^b	95.4	5.28 d (5.6)/5.14 d (5.6)	95.0
3	7.53 s	151.0	7.54 s	151.4	7.51 s	151.7
4		112.0		112.0		112.1
5	3.24 ^b	33.0	3.26 m	32.0	3.19 ^b	32.5
6a	2.36 m	30.0	2.38 m	30.6	2.32 m	30.4
6b	1.29 m		1.49		1.40 m	
7a	1.70 m ^b	39.0	1.63 ^b	41.4	1.68 br t (7.6)	39.3
7b	1.70 m ^b		1.63 ^b		1.63 br t (7.3)	
8		79.9		79.6		79.6
9	2.15 dd (5.5, 4.0)	51.0	2.16 m	51.7	2.15 m	51.1
10	1.32 s	24.0	1.34 s	24.5	1.30 s	24.1
11		167.4		167.5		167.2
glc-1'	4.73 d (7.7)	99.0	4.73 d (8.0)	99.3	4.71 d (7.8)/4.70 d (7.8)	99.0
2'	3.23 ^b	74.0	3.24 br t (9.0)	74.4	3.19 ^b	74.2
3'	3.39 t (9.5)	77.0	3.41 t (9.5)	77.5	3.40 t (9.5)	77.0
4'	3.37 t (9.5)	70.5	3.38 t (9.5)	71.3	3.35 ^b	71.0
5'	3.54 m	75.0	3.54 m	75.3	3.56 m/3.53 m	75.7
6'a	4.50 dd (12.0, 2.5)	63.3	4.53 dd (12.0, 3.0)	63.8	4.55 dd (11.5, 2.0)/4.51 dd (12.0, 2.0)	63.6
6'b	4.30 dd (12.0, 5.0)		4.30 dd (12.0, 5.0)		4.39 (12.0, 5.8)/4.33 dd (12.5, 6.0)	
1''		168.0		167.9		
2''		128.0		127.0		
3''	6.78 br t (7.6)	142.7	6.81 br t (7.6)	144.0		
H ₂ -4''	2.32 m	27.0	2.26 m	24.1		
H ₂ -5''	2.22 br t (7.5)	30.7	1.71 m	39.7		
6''		138.0		72.2		
7''	5.44 t (5.5)	125.8	5.94 dd (17.0, 10.0)	145.0		
8''a	4.07 d (7.0) ^b	58.1	5.25 ^b	112.1		
8''b	4.07 d (7.0) ^b		5.08 br d (10.0)			
9''	1.86 s	11.5	1.86 s	12.0		
10''	1.76 s	23.2	1.30 s	27.0		
<i>trans</i> 1''						125.2
2''/6''					7.45 d (8.0)	130.9
3''/5''					6.78 d (8.0)	115.5
4''						160.0
7''					7.68 d (16.0)	146.7
8''					6.35 d (16.0)	114.6
9''						167.9
<i>cis</i> 1''						126.5
2''/6''					7.66 d (8.0)	133.7
3''/5''					6.76 d (8.0)	115.8
4''						159.0
7''					6.87 d (12.0)	145.2
8''					5.77 d (12.0)	115.8
9''						167.2
fru-1a'''	4.05 d (12.0)	61.3	4.07 ^b	61.8	4.09 d (12.0)/4.07 d (12.0)	61.4
1b'''	3.69 ^b		3.70 ^b		3.60 ^b	
2'''		98.0		97.8		97.0
3'''	3.88 d (10.0)	68.0	3.90 d (10.0)	68.4	3.90 d (9.8)/3.88 d (10.0)	68.7
4'''	4.02 dd (10.0, 4.0)	69.0	4.04 ^b	69.0	4.00 m	69.0
5'''	5.13 m	72.2	5.15 m	72.0	5.12 m	72.6
6'''a	3.70 ^b	65.0	3.71 ^b	65.2	3.71 dd (16.0, 12.0)/3.69 dd (16.0, 12.0)	65.0
6'''b	3.49 br t (10.0)		3.51 br t (11.0)		3.46 dd (16.0, 5.0)	

^aSpectra were run in methanol-*d*₄ at 600 MHz (¹H) and 150 MHz (¹³C) for **8** and **10**, at 500 MHz (¹H) and 125 MHz (¹³C) for **9**. *J* values are in parentheses and reported in Hz; chemical shifts are given in ppm; assignments were confirmed by COSY, 1D-TOCSY, HSQC, and HMBC experiments.

^bOverlapped signal.

TOC Graphic



6-*O*-menthafolylmussaenosidic acid-11-(5-*O*-β-D-fructopyranosyl) ester